Talanta 106 (2013) 388–393

Contents lists available at SciVerse ScienceDirect

Talanta

journal homepage: www.elsevier.com/locate/talanta

Ultra-fast separation of infectious disease-related small DNA molecules by single- and multi-channel microchip electrophoresis

Peng Zhang [a], He Nan [a], Mi-Jin Lee [b], Seong Ho Kang [a,*]

[a] Department of Applied Chemistry, Kyung Hee University, Yongin-si, Gyeonggi-do 446-701, Republic of Korea
[b] Neodin Veterinary Science Institute, Seoul 140-240, Republic of Korea

ARTICLE INFO

Article history:
Received 12 December 2012
Received in revised form
9 January 2013
Accepted 10 January 2013
Available online 24 January 2013

Keywords:
Feline infectious peritonitis (FIP) virus
Microchip electrophoresis
Ultra-fast separation
Single- and multi-channel

ABSTRACT

An ultra-fast and precise microchip electrophoresis (ME) method was developed for the separation of infectious disease-related small DNA molecules. As a model of infectious disease-related small DNA molecules, the spike glycoprotein (S) gene of the *Feline infectious peritonitis* (FIP) virus was amplified using reverse transcript polymerase chain reaction. The amplified product of the FIP virus (223-bp) was analyzed within 10 s by single-channel ME under a sieving gel of 0.3% poly(ethylene oxide) (M_r=8,000,000) in 1x TBE buffer (pH 8.33) and a short effective channel length of 1.3 cm with a programmed step electric field strength (PSEFS) condition as follows: 470.6 V/cm for 9 s, 294.1 V/cm 1.5 s, and 470.6 V/cm for 9.5 s. The single-channel ME/PSEFS method was 50 times faster than that obtained with conventional slab gel electrophoresis. When the single-channel ME method was applied to a multi-channel ME for high-throughput screening, the precision of migration time and peak area showed standard deviations of less than 1.0% without any loss of resolving power. The ME assay technique provides a simple, precise and accurate method for ultra-fast analysis of infectious disease-related DNA under 400-bp.

1. Introduction

Following the seminal report by Manz et al., microchip electrophoresis (ME) has become a powerful technique in bio-analysis, especially for DNA and protein separation due to its analytical throughput and requirements for speed, small reagent volume, automation, miniaturization, and other advantages [1–5]. One significant advantage of ME is its high speed compared with conventional slab gel electrophoresis (SGE) and capillary electrophoresis (CE). The fast separation of DNA molecules is a critical technique in bio-analysis, especially in the clinical diagnosis of highly infectious diseases. ME separation methods used in detection of infectious diseases have been reported, with the output of results achieved in a matter of a few minutes [6–10]. Indeed, many studies have reported decreased separation times of given DNA molecules of around 1 min [11–14]. Development of faster and more precise methods that can separate and detect small DNA molecules in seconds is exigent for diagnosis of highly infectious diseases.

Feline Infectious Peritonitis (FIP), caused by the FIP virus, is one of the most severe infectious diseases of Felidae [15,16]. FIP tends to occur most frequently in catteries and multiple-cat households [17]. The high infectivity and large spread (up to 100% of cats in a multi-cat environment shed the virus) causes tremendous damage in cat communities [18]. In recent years, various protein- and gene-based detection methods have been used in clinical and laboratorial diagnosis of FIP [19–34]. However, protein-based methods such as serology tests, enzyme-linked immunosorbent assay (ELISA), and immunohistochemistry tests do not provide sufficiently accurate results [24,25]. In comparison, while gene detection methods based on reverse transcript polymerase chain reaction (RT-PCR) assays are able to accurately detect FIP virus [26–33], current RT-PCR methods continue to rely heavily on SGE analysis, which is both time and labor expensive [31]. Even though real-time RT-PCR methods may decrease analysis time, it requires special thermo cyclers equipped with an expensive sensitive camera and a well-designed primer [32,33]. Lastly, the biochip method based on microarray as another method to analyze RT-PCR products of FIP virus is complex and highly priced [34].

In this study, we developed an ultra-fast and precise ME separation method using PSEFS with a laser-induced fluorescence detector to analyze infectious disease-related DNA under 400-bp (i.e., S gene of FIP virus). Various separation parameters such as the sieving matrix, the effective length, and the electric field strength were discussed for faster detection without loss of resolution. As a proof of concept, the single-channel ME method was applied to a multi-channel ME system to demonstrate the feasibility of application for high-throughput screening.

* Corresponding author. Tel.: +8231 201 3349; fax: +8231 201 2340.
E-mail address: shkang@khu.ac.kr (S.H. Kang).

0039-9140/$ - see front matter © 2013 Elsevier B.V. All rights reserved.
http://dx.doi.org/10.1016/j.talanta.2013.01.030

2. Experimental

2.1. Reagents and materials

1x TBE buffer (0.089 M Tris, 0.089 M borate, and 0.002 M EDTA, pH 8.33) and 1xTAE buffer (0.04 M Tris-acetate, 0.001 M EDTA, pH 8.33) were prepared by dissolving a premixed powder (Ameresco, USA) in ultra-pure water. The dynamic coating matrix of the microchip was made by dissolving 1.0% w/v poly(vinyl pyrolidone) (PVP, M_r=1,000,000) (Ployscience, England) in a 1x TBE buffer with 0.5 ppm ethidium bromide (EtBr) (Sigma Chemicals, USA). The PVP solution was shaken for ~5 min to dissolve the PVP completely, which was then left to stand for 2 h to remove any bubbles. The poly(ethylene oxide) (PEO, M_r=8,000,000) (Sigma) solution used as sieving matrix was made by dissolving PEO in a 1x TBE buffer with 0.5 ppm EtBr. The PEO solution was stirred overnight to dissolve the polymer and to remove any bubbles.

2.2. Preparation of clinical samples

FIP virus samples were acquired from the Neodin Veterinary Science Institute (Seoul, Korea). Viral RNA was extracted from specimens using a Viral Nucleic Acid Extraction Kit II (Geneaid Biotech Ltd., Taipei, Taiwan) according to the manufacturer's instructions as follows: briefly, a 200-μL FIP virus sample was treated with a 400-μL lysis buffer (Geneaid, Taiwan) and then incubated at room temperature for 10 min. After incubation, the sample was treated with a 450-μL AD buffer (Geneaid, Taiwan) and centrifuged at 15,000 rpm for 1 min. The flow-through was then discarded and the sample was washed with a 400-μL W1 buffer (Geneaid, Taiwan). The remaining lysate was separated and dried before nucleic acid elution with 50 μl RNase-Free water (Geneaid, Taiwan). Lastly, the purified nucleic acid was eluted by centrifugation at 15,000 rpm for 1 min.

2.3. Reverse transcript polymerase chain reaction

For amplification of the spike glycoprotein (S) gene of the FIP virus, forward (5′-TGA GTT ATA AGG CAA CCC GAT G-3′) and reverse (5′-GAT CCA GAC GTT AGC TCT TCC A-3′) primers were used as described previously [35]. The amplification conditions for RT-PCR consisted of reverse transcription at 42 °C for 30 min, initial denaturation at 94 °C for 5 min, followed by 40 cycles of denaturation at 94 °C for 30 s, annealing at 54 °C for 30 s, and extension at 72 °C for 40 s.

2.4. Slab gel electrophoresis

Amplified DNA molecules were identified by SGE in 1.5% agarose gel (Sigma) using a 1x TAE buffer, stained with EtBr, and then photographed using a still video documentation system (CoreBio MC2000, Korea). The presence of a 223-bp DNA band was recorded as a positive result. The sizes of the DNA products were determined relative to a 100-bp DNA ladder.

2.5. Single- and multi-channel microchip electrophoresis

Single-channel microchip electrophoresis was performed on a DBCE-100 Microchip CE System (NanoEntek, Korea) (Fig. 1A) equipped with a diode-pumped solid-state laser (excitation at 532 nm; Power Technology, USA) and a high-voltage device (DBHV-100, NanoEntek, Korea). The glass single-channel microchip was purchased from Micralyne (MCBF4-TT100, Micralyne, Canada). The injection design was a double-T channel with a 100-μm offset. The chip channel was 50 μm wide and 20 μm deep. The reservoirs were 2.0 mm in diameter and 1.0 mm deep. The injection channel length (from reservoir 2 to 4) was 8.0 mm. The separation channel (from reservoir 1 to 3) was 8.5 cm long. Detection was performed at 1.0–4.5 cm from the injection-T (Fig. 1B).

A lab-built LIF detection system (Fig. 1C) was used for multi-channel ME. A diode-pumped solid-state laser (excitation at 532 nm; Shanghai Laser & Optics Century, China) was used for excitation. Two cylindrical lenses were used to focus the laser beam on the central part of the detection area of the multi-channel microchip. A microscope (IMT-2, Olympus, Japan) with an objective lens (10x/0.25 N.A.; Olympus, Japan) was used to collect and transmit the fluorescence signal from the analyte to the detector, which consisted of a charged-coupled device (CCD) detector (01-EXI-BLU-R-F-M-14-C, QImaging, Canada). A band-pass filter (35-5081, 600.0 ± 8.0 nm; Ealing Catalog, USA) was placed in front of the CCD camera to filter out irrelevant wavelengths. Detection region images from the CCD camera were analyzed using Image-Pro Plus (Media Cybernetics, Version 7.0) software to obtain fluorescence intensity curves. The glass multi-channel microchip (NanoEntek, Korea) had three channels (i, ii, and iii) with ten reservoirs on the cover glass. The chip channels were 50 μm wide and 10 μm deep and connected with reservoirs with a 2.0-mm diameter. The injection design of each channel was a double-T pattern. The length of the separation channel was 6.5 cm (Fig. 1D).

2.6. Electrophoretic separation in microchips

The PVP dynamic coating and PEO sieving matrix were filled hydrodynamically using a vacuum pump set at 8.67×10^4 Pa (EYELA A-3s vacuum aspirator, Japan) for ME reservoir 3 in Fig. 1B for 5 min, respectively. The sample (3.5 μL) was then pipetted into the sample inlet reservoir (reservoir 4 in Fig. 1B) of the microchip and injected to the injection-T region using a conventional electrokinetic injection method. The injection potential was set as 480 V at sample outlet reservoir 2 followed by grounding sample inlet reservoir 4 for 60 s.

The applied separation electric field strength was step controlled and adjusted in the time domain by DBMA-100 software to range from 40 to 470.6 V/cm between reservoirs 1 and 3. During separation, the maintained voltage (the potential difference between reservoirs 2 and 4) was applied properly according to the separation voltage. After each run, the microchannel was rinsed with water followed by a running buffer for 10 min each.

2.7. Programmed step electric field strength (PSEFS)

The PSEFS separation was optimized as follows. First, the constant electric field strength in the range of 100–500 V/cm was used to separate all the DNA molecules of the DNA ladder. After the separation, the determination of whether PSEFS or constant electric field strength provided the best result was established. If PSEFS was chosen, we eliminated or decreased the portions of the gradient prior to the first DNA peak (200-bp) and following the last DNA peak (300-bp). Finally, if the separation in the second step was acceptable, the gradient time was decreased to reduce separation time. The PSEFS was programmed to give the best separation of the target DNA molecule (223-bp DNA) with more than 1.5 of resolution.

3. Results and discussion

3.1. Optimization of the single-channel ME separation

The aqueous solution of uncross-linked PEO was used as the sieving matrix. Even though a higher sieving matrix concentration can improve separation efficiency, it can also result in a longer migration time of the analyte (Supporting Information, Fig. S1A).

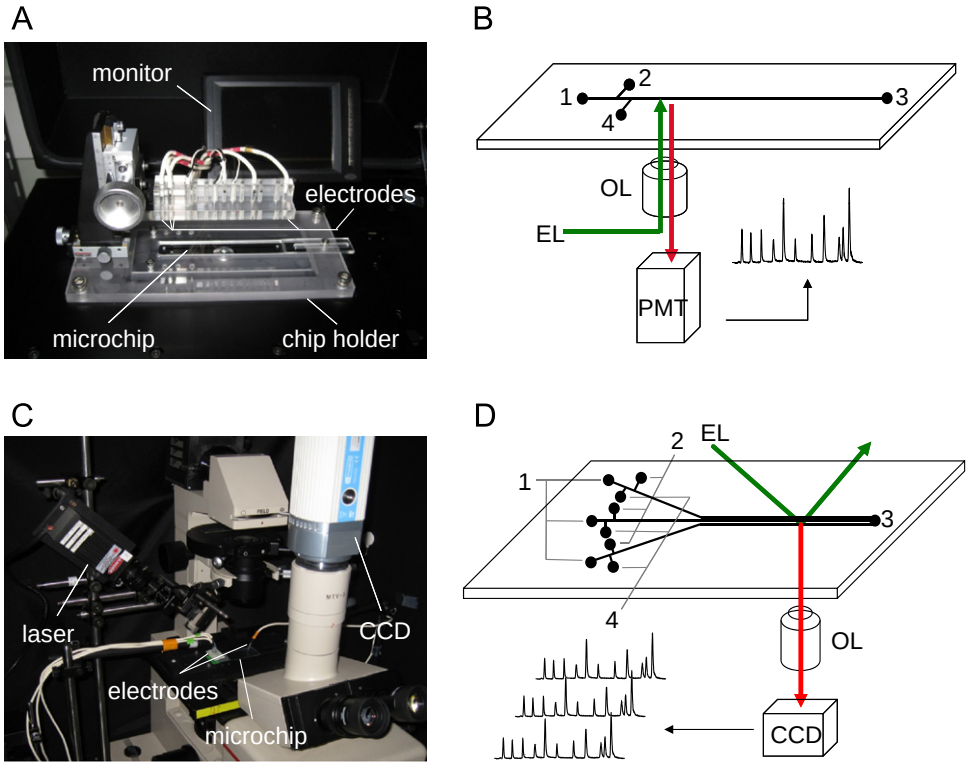

Fig. 1. Single- and multi-channel ME with laser induced fluorescence (LIF) detection systems. (A) Physical layout and (B) schematic diagram of the single-channel ME system. (C) Physical layout and (D) schematic diagram of the multi-channel ME system. Indication: EL, excitation light OL, objective lens; PMT, photomultiplier tube; CCD, charge-coupled device; reservoir 1, buffer inlet; reservoir 2, sample outlet; reservoir 3, buffer waste; reservoir 4 and sample inlet.

Furthermore, higher PEO concentrations resulted in numerous problems including bubble residue, increased difficulty, and time required to fill and clean microchannel blockage. Taking into consideration migration time, resolution, and operability, a PEO concentration of 0.3% was used as the optimum condition for the sieving matrix.

To confirm the migration behavior of DNA molecules in microchannels, the relationship between migration time and effective length was studied (Fig. 2A). We considered it noteworthy that, aside from the different slopes (index of migration velocity), neither the size of the DNA molecules (100-, 200-, 300-, 800-, and 1000-bp) nor the electric filed strength (129.4 V/cm and 470.6 V/cm) had an effect on linearity. We considered this to be due to the uniform motion performance of DNA molecules. Furthermore, this indicated the feasibility of using the high acceleration of DNA molecules and the possibility of short separation lengths to decrease migration time of analytes with high linearity, precision, and accuracy.

Even though recent theoretical studies of ME have reported that a high electric field is adequate for short effective lengths, the electrophoretic mobility of DNA molecules under high electric fields becomes field-dependent [36,37]. Here, we studied electric field strength as a function of migration time differences ($T_B - T_A$) and separation efficiency (N) for given DNA molecules to establish the effect of electric field strength to resolution. With increasing electric field strength from 0 to 400 V/cm, the difference of migration time ($T_B - T_A$) for given DNA molecules decreased dramatically, especially for large DNA molecules (800- and 1000-bp) (Fig. 2B). For small DNA molecules (100-, 200- and 300-bp), N increased at a relatively low electric field strength range (<350 V/cm). Conversely, high electric fields (>350 V/cm) decreased N dramatically. Thus, the N of large DNA molecules (800- and 1000-bp) decreased with increasing electric field strength (Fig. 2C).

Classical electrophoresis theory considers that Joule heat affects migration performance primarily as indicated in Eq. (1) [36].

$$t_{\text{anal}} = \frac{L}{\mu_2 E} = \frac{8R_s^2 B + 4\sqrt{4R_s^4 B^2 + \mu_{rel}^2 R_s^2 A}}{\mu_{\text{rel}}^2 \mu_2 E} \tag{1}$$

where

$$A = \sigma_{\text{inj}}^2 + \sigma_{\text{det}}^2 \tag{1a}$$

$$B = 2\frac{D_a}{\mu E} + \frac{D_{\text{heat}}}{\mu E} \tag{1b}$$

Surprisingly, the tendencies of migration time curves for specific DNA molecules at a different electric field strength in our studies (Supporting Information, Fig. S1B) was highly correlated with Eq. (1) without D_{heat} (the effective gradient broadening coefficient). However, D_{heat} could not be omitted entirely, since the electroosmotic flow (EOF) was significantly inhibited in channels coated with PVP, and resulted in dramatically decreased channel current. In addition, we observed that the 50×20 μm microchip channels were able to eliminate heat effectively.

Consequently, we observed a low separation efficiency of given DNA molecules at a high electric field, which was primarily attributed to conformation aberration and entanglement of DNA molecules and the sieving matrix. Specifically, larger DNA molecules (>400 bp) experience entanglement easier, and such intermolecular affects tend to be magnified by high strength electric fields. Therefore, adjustment of the electric field (to program the field strength to change during analysis) is required for ultra-fast identification of given DNA molecules with high precision and accuracy.

The electric field distribution pattern had a significant influence on baseline readings, and therefore must be designed carefully. Due

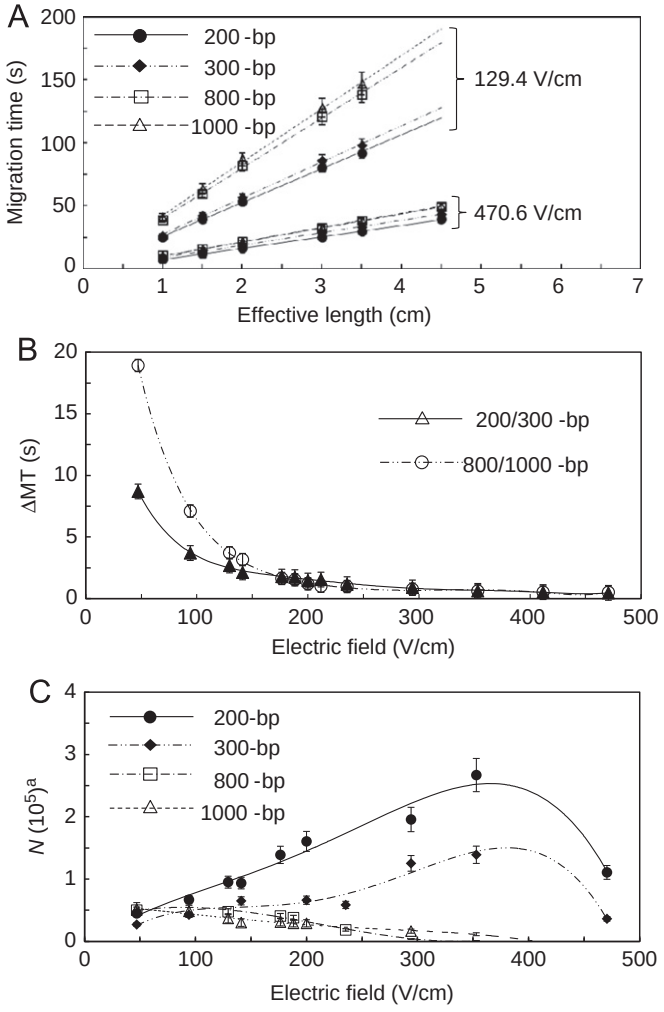

Fig. 2. (A) Migration time of DNA molecules as a function of effective length at different applied electric fields, (B) difference of migration times (ΔMT), and (C) separation efficiency (N) of given DNA molecules as a function of the applied electric field strength. Running buffer, 1x TBE buffer (pH 8.33) with 0.5 ppm EtBr; coating matrix, 1.0% PVP (M_r=1,000,000); sieving matrix, 0.3% PEO (M_r=8,000,000); sample concentration, 14.4 ng/μL; single-channel ME. Vertical bars represent the standard deviations of the respective means (n=5). [a]$N=5.54\times$(migration time/peak width at half of the peak height)^2.

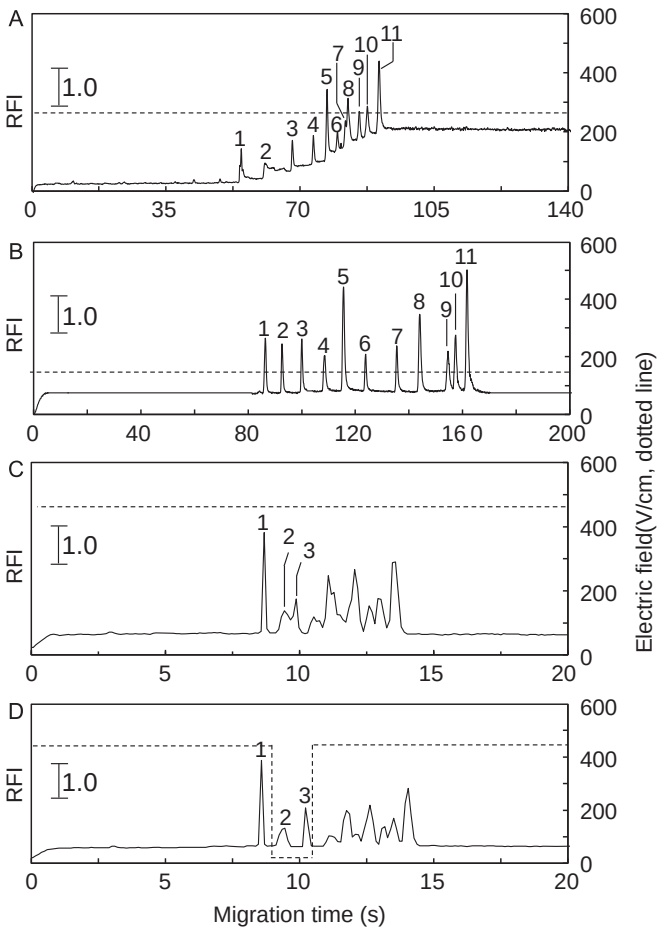

Fig. 3. Electropherograms of the 100-bp DNA ladder in the ME system. (A) Maintenance voltage un-matched with separation voltage, (B) matched voltage with low constant electric field strength (LCEFS) for separation, (C) matched voltage with high constant electric field strength (HCEFS), and (D) matched voltage with programmed step electric field strength (PSEFS) for separation. Separation conditions: running buffer, 1x TBE buffer (pH 8.33) with 0.5 ppm EtBr; coating matrix, 1.0% PVP (M_r=1,000,000); sieving matrix, 0.3% PEO (M_r=8,000,000); sample concentration, 14.4 ng/μL; applied separation electric field, (A) 294.1 V/cm, (B) 129.4 V/cm, (C) 470.6 V/cm from 0 to 9 s, 294.1 V/cm form 9 to 10.5 s, 470.6 V/cm from 10.5 to 20 s. Peaks: 1=100-bp, 2=200-bp, 3=300-bp, 4=400-bp, 5=500-bp, 6=600-bp, 7=800-bp, 8=1000-bp, 9=1500-bp, 10=2000-bp, 11=3000-bp. RFI, relative fluorescence intensity.

to our distinctive chip design and electrokinetic sample injection mode, the electric field pattern depended not only on the applied separation voltage (potential difference between reservoirs 1 and 3) but also on the maintenance voltage, which was applied to reservoirs 2 and 4. The optimum ratio of separation voltage to maintain voltage was approximately 10; unmatched maintenance voltages resulted in a staircase baseline drift (Fig. 3A).

3.2. Fast detection of specific DNA molecules by single-channel ME with PSEFS

Conditions for PSEFS were optimized as follows. First, we determined the low constant electric field strength required for separation of all DNA molecules (Fig. 3B). Secondly, we applied a high strength constant electric field (Fig. 3C). Next, we decreased the electric field strength at specific domains. Finally, if the separation achieved during the third step was deemed acceptable, we reduced the gradient time. By applying high constant electric field strength in non-related region of DNA ladder, the DNA molecules across the separation channel with high speed which could decrease the analysis time remarkably. As a contrast, the relative low electric field which was applied in interested region can decrease the migration speed of specific DNA molecules to increase the separation efficiency and resolution. Thus, as programming the step electric field strength in time domain, the ultra-fast separation of specific small DNA molecules without any loss of resolution was achieved (Fig. 3D). After optimization, the best PSEFS condition for the fast separation of 200- and 300-bp DNA molecules was determined to be 470.6 V/cm for 9 s, followed by 294.1 V/cm for 1.5 s, and finished with 470.6 V/cm 9.5 s (Fig. 3D). The migration times of 200- and 300-bp DNA were 9.3 ± 0.3 s and 10.2 ± 0.2 s, respectively, and the resolution of 200/300-bp DNA molecules was 3.96 ± 0.06. Together, these results indicate that the PSEFS method was capable of achieving ultra-fast separation speed without any loss of resolving power.

3.3. Multi-channel ME for high-throughput screening

To increase the throughput, the PSEFS protocol of 692.3 V/cm from 0 to 21 s, 384.6 V/cm from 21 to 26 s, and 692.3 V/cm from 26 to 50 s was applied to a multi-channel ME system to concurrently detect a DNA ladder and analyte (223-bp of FIP virus DNA).

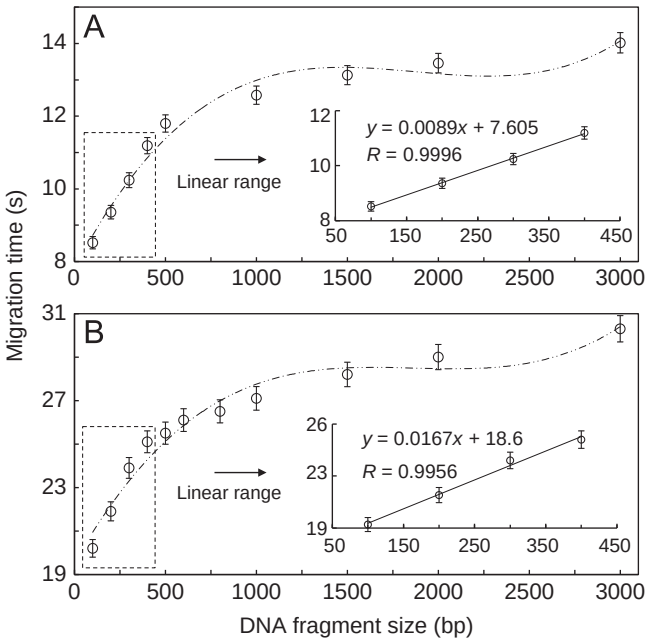

Fig. 4. Calibration curve of migration time as a function of the molecular length of 100-bp DNA ladder (bp) in (A) single-channel ME and (B) multi-channel ME. Inset: linearity of the target detection range. The separation and detection conditions are the same as shown in Fig. 3. Vertical bars represent the standard deviations of the respective means (n=5).

Instead of a photomultiplier tube (PMT) detector, a CCD camera was used in the multi-channel ME system to directly record real-time fluorescent images of EtBr intercalated DNA molecules in all microchip channels (Supporting information, Fig. S2). According to the design of the multi-channel chip and detection system, the effective length was set as 3.5 cm. After operation and signal processing, the three samples (100-bp DNA ladder) were separated simultaneously (electropherogram not shown). The migration times of the 200- and 300-bp DNA molecules were 21.9 ± 0.3 s and 23.9 ± 0.4 s, respectively. The resolution of the 200/300-bp DNA molecules was 4.0 ± 0.06.

Calibration curves were fitted according to the migration times of different DNA molecule length (bp) in single- and multi-channel ME (Fig. 4). The correlation coefficients (R) of the detection region ($\leq$400-bp) in single-channel and multi-channel systems were 0.9996 and 0.9956, respectively, indicating that our PSEFS protocol provided excellent linearity for small DNA molecules. Furthermore, the approach described in this study may be a simple and powerful method for clinical applications aimed at the analysis of infectious disease-based small DNA molecules under 400-bp with high speed and accuracy.

3.4. Clinical applications

Optimized PSEFS protocols were applied to single- and multi-channel MEs to detect FIP virus DNA. The sizes of sample DNA molecules amplified from the FIP clinical sample virus were determined *via* RT-PCR. RT-PCR products were verified as 223-bp products by SGE (Fig. 5A). Samples amplified from FIP infected cats (positive sample) were diagnosed at 9.6 ± 0.2 s by the single-channel ME method (Fig. 5B). To verify the accuracy of the method, we evaluated samples amplified from non-infected cats (negative control) and blank samples were in parallel.

To achieve high throughput, the DNA ladder and FIP infected and non-infected samples were analyzed in three channels simultaneously by multi-channel ME based on PSEFS. After using PSEFS in multi-channel ME, the FIP infected sample was analyzed

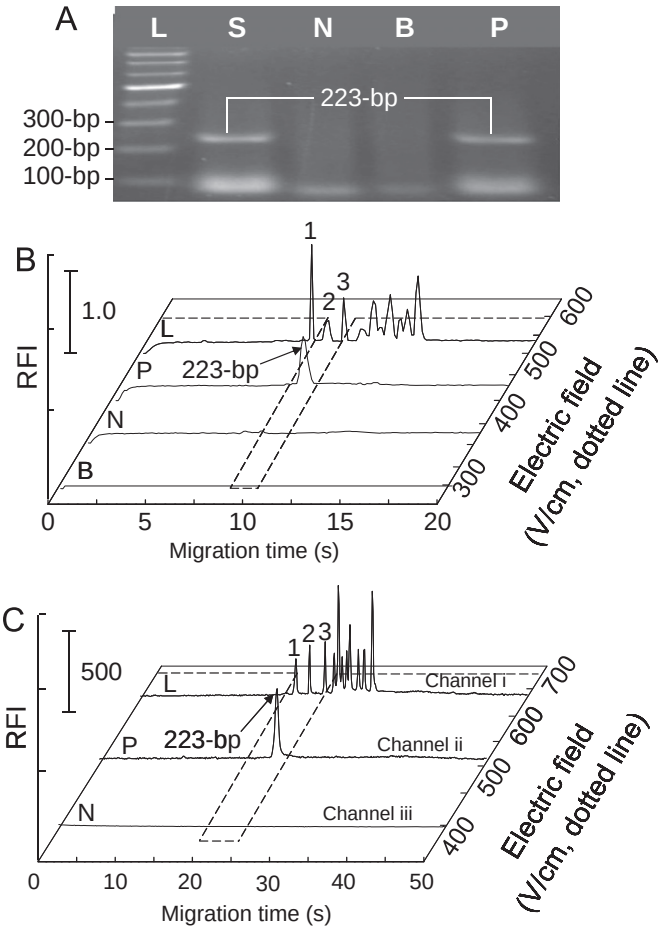

Fig. 5. (A) Representative SGE electropherograms of amplified PCR products for the FIP virus from blood of infected cats diagnosed using PSEFS in (B) single-channel ME and (C) multi-channel ME. SGE conditions: 1.5% agarose gel matrix in 1x TAE buffer (0.04 M Tris-acetate, 0.001 M EDTA, pH 8.33); applied voltage, 150 V for 60 min; temperature, ambient. ME condition, running buffer, 1x TBE buffer (pH 8.33) with 0.5 ppm EtBr; coating matrix, 1.0% PVP (M_r=1,000,000); sieving matrix, 0.3% PEO (M_r=8,000,000); microchip effective length, (B) 1.3 cm, (C) 3.5 cm; PSEFS, (B) 470.6 V/cm from 0 to 9 s, 294.1 V/cm form 9 to 10.5 s, 470.6 V/cm from 10.5 to 20 s, (C) 692.3 V/cm from 0 to 21 s, 384.6 V/cm form 21 to 26 s, 692.3 V/cm from 26 to 50 s. L=DNA ladder, S=sample, N=negative control, B=blank control, P=positive control. Peaks: 1=100-bp, 2=200-bp, 3=300-bp. RFI, relative fluorescence intensity.

at 22.4 ± 0.3 s (Fig. 5C), 15 times faster than the conventional SGE method.

We achieved good reproducibility and accuracy with respect to migration time and peak area of the DNA ladder and positive samples at the 95% confidence level (Table 1). These results indicated that our protocol was not only fast, but also highly precise and accurate.

4. Conclusions

An ultra-fast detection strategy for infectious disease-related small DNA molecules ($\leq$400-bp DNA) based on microchip gel electrophoretic separation with PSEFS was investigated. By studying the sieving matrix, effective length, and electric field strength of single-ME system, the PSEFS method was developed and optimized to separate the 200- and 300-bp DNA molecules among a 100-bp DNA ladder within 10 s without any loss of resolution. Furthermore, the PSEFS tactics were successfully applied to a multi-channel ME system, demonstrating the feasibility of high-throughput ME screening.

Table 1
Comparison of migration time and peak area of specific DNA molecules and RT-PCR products of the FIP virus by applying PSEFS in single- and multi-channel ME.

Sample	Single-channel ME	Multi-channel ME
	Migration time (s)/peak area	Migration time (s)/peak area
200-bp	$9.3 \pm 0.3/0.282 \pm 0.01$	$21.9 \pm 0.3/208.92 \pm 0.4$
300-bp	$10.2 \pm 0.2/0.288 \pm 0.03$	$23.9 \pm 0.4/244.14 \pm 0.3$
FIPV infected	$9.6 \pm 0.2/0.838 \pm 0.04$	$22.4 \pm 0.3/480.66 \pm 0.3$
FIPV non-infected	–/–	–/–
Blank	–/–	–/–

Applied separation conditions are shown in Fig. 5. The data show mean ± standard deviation ($n=5$). FIPV=FIP virus.

Finally, the RT-PCR product of the FIP virus (223-bp) was analyzed by single- and multi-channel channel ME with PSEFS. The RT-PCR products of FIP virus were detected within 9.6 ± 0.2 s with a single-channel ME method, which is 50 times faster than conventional SGE methods. Furthermore, multi-channel ME with PSEFS provided high throughput screening ability with a 22.4 ± 0.3 s separation time, which is 15 times faster than SGE methods. Additionally, the excellent reproducibility and accuracy achieved with PSEFS in single- and multi-channel ME experiments were taken as an indication of its essentialness as an assay technique for ultra-fast analysis of infectious disease-related small DNA molecules ($\leq$ 400-bp).

Acknowledgments

This research was supported by the National Research Foundation of Korea (NRF) grant funded by the Korea Government (MEST) (No. 2012R1A2A2A01013466).

Appendix A. Supporting information

Supplementary data associated with this article can be found in the online version at http://dx.doi.org/10.1016/j.talanta.2013.01.030.

References

[1] A. Manz, D.J. Harrison, E.M.J. Verpoorte, J.C. Fettinger, A. Paulus, H. Luedi, H.M. Widmer, J. Chromatogr. 593 (1992) 253–258.
[2] L. Zhang, F. Dang, Y. Baba, J. Pharm. Biomed. Anal. 30 (2003) 1645–1654.
[3] A.T. Woolley, R.A. Mathies, Anal. Chem. 67 (1995) 3676–3680.
[4] D. Schmalzing, A. Adourian, L. Koutny, L. Ziaugra, P. Matsudaira, D. Ehrlich, Anal. Chem. 70 (1998) 2303–2310.
[5] C. Backhouse, M. Caamano, F. Oaks, E. Nordman, A. Carrillo, B. Johnson, S. Bay, Electrophoresis 21 (2000) 150–156.
[6] L.C. Waters, S.C. Jacobson, N. Kroutchinina, J. Khandurina, R.S. Foote, J.M. Ramsey, Anal. Chem. 70 (1998) 158–162.
[7] L.C. Waters, S.C. Jacobson, N. Kroutchinina, J. Khandurina, R.S. Foote, J.M. Ramsey, Anal. Chem. 70 (1998) 5172–5176.
[8] Y.-H. Chen, W.-C. Wang, K.-C. Young, T.-Y. Chang, S.-H. Chen, Clin. Chem. 45 (1999) 1938–1943.
[9] X. Zhou, D. Liu, R. Zhong, Z. Dai, D. Wu, H. Wang, Y. Du, Z. Xia, L. Zhang, X. Mei, B. Lin, Electrophoresis 25 (2004) 3032–3039.
[10] E.T. Lagally, J.R. Scherer, R.G. Blazej, N.M. Toriello, B.A. Diep, M. Ramchandani, G.F. Sensabaugh, L.W. Riley, R.A. Mathies, Anal. Chem. 76 (2004) 3162–3170.
[11] S.H. Kang, M. Park, K. Cho, Electrophoresis 26 (2005) 3179–3184.
[12] K.S. Kumar, S.H. Kang, Electrophoresis 28 (2007) 4247–4254.
[13] H.G. Lee, K.S. Kumar, J.-R. Soh, Y.-S. Cha, S.H. Kang, Anal. Chim. Acta 619 (2008) 94–100.
[14] E.N. Fung, E.S. Yeung, Anal. Chem. 67 (1995) 1913–1919.
[15] J. Holzworth, Cornell Vet. 53 (1963) 157–160.
[16] K.J. O'Reilly, B. Fishman, L.M. Hitchcock, Vet. Rec. 104 (1979) 348.
[17] J.E. Foley, A. Poland, J. Carlson, N.C. Pedersen, J. Am. Vet. Med. Assoc. 210 (1997) 1307–1312.
[18] N.C. Pedersen, Feline Pract. 23 (1995) 7–20.
[19] K. Hartmann, C. Binder, J. Hirschberger, D. Cole, M. Reinacher, S. Schroo, J. Frost, H. Egberink, H. Lutz, W. Hermanns, J. Vet. Intern. Med. 17 (2003) 781–790.
[20] S. Duthie, P.D. Eckersall, D.D. Addie, C.E. Lawrence, O. Jarrett, Vet. Rec. 141 (1997) 299–303.
[21] S. Paltrinieri, P. Saverio, A. Giordano, G. Alessia, V. Tranquillo, T. Vito, S. Guazzetti, G. Stefano, J. Vet. Diagn. Invest. 19 (2007) 266–272.
[22] S. Paltrinieri, E. Gelain Maria, F. Ceciliani, M. Ribera Alba, M. Battilani, J. Feline Med. Surg. 10 (2008) 514–518.
[23] D. Addie Diane, A. McLachlan Shona, M. Golder, I. Ramsey, O. Jarrett, J. Feline Med. Surg. 6 (2004) 63–67.
[24] M.A. Kennedy, M. Abd-Eldaim, S.E. Zika, J.M. Mankin, S.A. Kania, Am. J. Vet. Res. 69 (2008) 1179–1182.
[25] K. Hartmann, Vet. Clin. North Am. Small Anim. Pract. 35 (2005) 39–79.
[26] S. Escutenaire, N. Mohamed, M. Isaksson, P. Thoren, B. Klingeborn, S. Belak, M. Berg, J. Blomberg, Arch. Virol. 152 (2007) 41–58.
[27] C. Dye, R. Helps Christopher, G.Siddell Stuart, J. Feline Med. Surg. 10 (2008) 167–174.
[28] A. Duarte, I. Veiga, L. Tavares, Vet. Microbiol. 138 (2009) 163–168.
[29] D.D. Addie, I.A.T. Schaap, L. Nicolson, O. Jarrett, J. Gen. Virol. 84 (2003) 2735–2744.
[30] S. Sharif, S. Arshad Siti, M. Hair-Bejo, R. Omar Abdul, A. Zeenathul Nazariah, S. Fong Lau, N.-A. Rahman, H. Arshad, S. Shamsudin, A.Isa Mohd-Kamarudin, Acta Vet. Scand. 52 (2010) 1.
[31] F.A. Simons, H. Vennema, J.E. Rofina, J.M. Pol, M.C. Horzinek, P.J.M. Rottier, H.F. Egberink, J. Virol. Methods 124 (2005) 111–116.
[32] C. Gibson, N. Parry, Vet. Med. 102 (2007) 375–379.
[33] K. Can-Sahna, V. Soydal Ataseven, D. Pinar, C.Oguzoglu Tuba, J. Feline Med. Surg. 9 (2007) 369–372.
[34] K. de Souza Luna Luciano, V. Heiser, N. Regamey, M. Panning, F. Drexler Jan, S. Mulangu, L. Poon, S. Baumgarte, J. Haijema Bert, L. Kaiser, C. Drosten, J. Clin. Microbiol. 45 (2007) 1049–1052.
[35] A. Alazawy, S.-S. Arshad, M. Hair-Bejo, A.-R. Omar, T.-A. Tengku-Ibrahim, F. Bande, A. Assumaidaee, Afr. J. Biotechnol. 11 (2012) 10451–10461.
[36] Y. Ni, X. Dou, S. Cheng, Y. Zhu, Electrophoresis 32 (2011) 238–245.
[37] D.H. Flint, R.E. Harrington, Biochemistry 11 (1972) 4858–4864.